Macular Choroidal Thickness Measured by Swept Source Optical Coherence Tomography in Eyes with Inferior Posterior Staphyloma

Abdallah A. Ellabban,[1,2] *Akitaka Tsujikawa,*[1] *Akiko Matsumoto,*[1,3] *Kenji Yamashiro,*[1] *Akio Oishi,*[1] *Sotaro Ooto,*[1] *Isao Nakata,*[1] *Yumiko Akagi-Kurashige,*[1] *Masahiro Miyake,*[1] *and Nagahisa Yoshimura*[1]

Purpose. To study the choroidal thickness in eyes with inferior posterior staphyloma (IPS) and to elucidate its role in the development of macular complications.

Methods. The macular area of 42 eyes of 32 patients with IPS was studied prospectively with swept source optical coherence tomography at 1050 nm. Using a raster scan protocol with 512 × 128 A-scans, we produced a macular choroidal thickness map (6 × 6-mm^2).

Results. Eyes with IPS showed relatively well-preserved choroid outside of the staphyloma but the inferior-nasal choroid within the staphyloma was thinned substantially. In addition, eyes with IPS often had a belt-shaped area with the thinnest choroid along the superior border of the staphyloma. As patient age increased, choroidal thinning progressed in the entire macular area. The macular choroidal thickness showed a close correlation with age ($R^2 = 0.506$, $P < 0.001$). On the superior border of the staphyloma, 13 eyes (30.9%) showed serous retinal detachment and/or pigment epithelial detachment without neovascularization, and eight (19.0%) showed neovascularization. Patients with neovascularization were older and had worse visual acuity ($P < 0.001$). Macular choroidal thickness in eyes with neovascular complications (76.5 ± 19.9 μm) was significantly reduced compared with that of eyes with no complication (133.0 ± 61.9 μm, $P = 0.035$).

Conclusions. Eyes with IPS showed marked choroidal thinning along the superior border of the staphyloma. Reduction of the choroidal thickness progressed with age and seemed to be involved in the development of neovascularization associated with the IPS. (*Invest Ophthalmol Vis Sci.* 2012;53:7735–7745) DOI:10.1167/iovs.12-9952

From the [1]Department of Ophthalmology and Visual Sciences, Kyoto University Graduate School of Medicine, Kyoto, Japan; the [2]Department of Ophthalmology, Suez Canal University, Faculty of Medicine, Ismailia, Egypt; and [3]Topcon Corporation, Tokyo, Japan.

Submitted for publication March 30, 2012; revised September 11 and 29, 2012; accepted October 21, 2012.

Disclosure: **A.A. Ellabban**, None; **A. Tsujikawa**, None; A. **Matsumoto**, Topcon Corporation (E); **K. Yamashiro**, None; **A. Oishi**, None; **S. Ooto**, None; **I. Nakata**, None; **Y. Akagi-Kurashige**, None; **M. Miyake**, None; **N. Yoshimura**, Topcon Corporation (F), Nidek (F, C), Canon (F)

Corresponding author: Akitaka Tsujikawa, Department of Ophthalmology, Kyoto University Graduate School of Medicine, Sakyo-ku, Kyoto 606-8507, Japan; tujikawa@kuhp.kyoto-u.ac.jp.

Investigative Ophthalmology & Visual Science, November 2012, Vol. 53, No. 12

Inferior posterior staphyloma (IPS) is one type of primary posterior staphyloma associated with myopia which was classified by Curtin.[1] IPS is often accompanied by tilted disc syndrome, peripapillary crescent, dysversion of retinal vessels, and, less often, visual field defects.[2–5] When the superior border of the staphyloma lies across the macula, it may be accompanied by macular complications, such as atrophy of the RPE, serous retinal detachment, choroidal neovascularization (CNV), or polypoidal choroidal vasculopathy (PCV).[6–13] Most eyes with serous retinal detachment associated with IPS have good visual function, but the development of CNV or PCV often results in a poor visual prognosis.[7]

A number of recent reports have shown that the choroid is involved in the pathogenesis of various ocular diseases.[14–21] In a previous report by Nakanishi et al.,[7] choroidal vascular disturbance, as evidenced by angiography, was suggested to be a possible mechanism for the development of macular complications in eyes with IPS. In a recent report on eyes with foveal serous retinal detachment from IPS, Maruko et al.[22] noted that foveal choroidal thinning may contribute to a focal disturbance in the choroidal circulation. Anatomic disturbances at the superior border of the staphyloma may lead to hemodynamic changes or mechanical forces on choroidal layers at the macula.[6,7] However, thus far there is little information available on the association between the choroidal changes in eyes with IPS and the development of neovascular complications.

Since Spaide et al.[23] introduced enhanced depth imaging based on optical coherence tomography (OCT) technology, changes in choroidal thickness have been reported in various chorioretinal diseases. In most of these studies, the choroidal thickness was measured at the foveal center or, sometimes, at several measurement points.[14–17,19,20,24–29] In contrast, swept source OCT, which has a light source of a longer wavelength, allows long-penetration imaging with high acquisition speed and contrast.[30,31] With these advantages, it can produce three-dimensional images of the entire choroid. In the study described herein, using swept source OCT at 1050 nm, we examined three-dimensionally the macular area of eyes with IPS and produced macular choroidal thickness maps. Using these measurements, we then studied changes in the choroid of eyes with IPS to see if there was any association with macular complications, especially with neovascular complications.

Patients and Methods

This prospective study consisted of 42 eyes of 32 patients with IPS, of which the superior edge was lying across the macula. The macular area of the study subjects was examined with a prototype swept source

OCT system at Kyoto University Hospital between August 2010 and November 2011. The diagnosis of IPS was based on fundus photography, dilated binocular indirect ophthalmoscopy, and slit lamp biomicroscopy with a contact lens. Vertical scans of OCT were used to confirm that the border of the inferior staphyloma lay across the macula. The Institutional Review Board and Ethics Committee of Kyoto University approved this study. All subjects were treated in accordance with the Declaration of Helsinki. Written informed consent for research participation was obtained from each subject before examination.

All subjects underwent a comprehensive ocular examination, including autorefractometry (ARK1; Nidek, Gamagori, Japan), best-corrected visual acuity (VA) measurement with a 5-meter Landolt chart, axial length measurement using ocular biometry (IOLMaster; Carl Zeiss Meditec, Jena, Germany), slit lamp examination, intraocular pressure measurement, dilated color fundus photography (TRC50LX; Topcon Corp., Tokyo, Japan), and prototype swept source OCT examination. All eyes with macular complications underwent simultaneous fluorescein angiography and indocyanine green angiography using HRA+OCT (Spectralis; Heidelberg Engineering, Heidelberg, Germany). Eyes with poor images due to unstable fixation or opaque media (e.g., cataracts or corneal opacity) were excluded from the study. Eyes were also excluded if they had a preexisting ocular disease or a history of ocular surgery, except for cataract surgery.

Eligible eyes with IPS were classified into three groups based on the associated complications. Eyes with IPS without any evidence of exudative changes or CNV associated with IPS were classified as group 1. Eyes that showed serous retinal detachment and/or pigment epithelial detachment in the macular area without CNV were classified as group 2. In this group, each eye was carefully examined by angiography to confirm the absence of CNV or PCV. Eyes that showed neovascular complications, including CNV and PCV, were classified as group 3. The diagnosis of CNV was based on the presence of leakage on fluorescein angiography and intraretinal or subretinal fluid on OCT. The diagnostic criteria for PCV were based on indocyanine green angiography, which showed a branching vascular network that terminated in polypoidal swelling.

Swept Source OCT System and Scan Protocols

The prototype swept source OCT system (Topcon Corp.) used in the current study has been described previously.[30] This swept source OCT uses a light source of a wavelength-sweeping laser centered at 1050 nm with 100,000 Hz repetition rate. The optical power incident on the eye by the current swept source laser system is less than 1 mW, which is well below the safety requirements of the American National Standards Institute for this class of laser. This prototype swept source OCT system has a depth in the scan window of 2.6 mm.

Swept source OCT examinations of the eligible subjects were performed by trained examiners after pupil dilation. A three-dimensional imaging data set was acquired by using a raster scan protocol of 512 (horizontal) × 128 (vertical) A-scans per data set (total 65,536 axial scans/data set) in 0.8 seconds. Each raster scan covered a 6 × 6-mm^2 area centered on the fovea, which was confirmed by internal fixation and by a fundus camera built into the swept source OCT system. To reduce speckle noise, each image was enhanced by the weighted moving average of three consecutive original images. In four eyes of patients, we could not obtain data on the outer inferior sector because the obtained images were partially inverted due to a limit of the scan window of the OCT; these data were excluded from analysis.

In all subjects, multiaveraged line scans of 12 mm, horizontal and vertical, composed by averaging 50 scans, were obtained. The 50 single images were registered and averaged by software to create an averaged single image. The vertical line scan was centered on the fovea while the horizontal line scan was centered on the midpoint between the fovea and optic disc.

Table 1. Choroidal Thickness and Volumes of Eyes with Inferior Posterior Staphyloma

Number of eyes	42
Sex (male/female)	9/23
Tilted disc (%)	35 (83.3%)
Age, y	67.8 ± 11.3
Axial length, mm	25.00 ± 1.52
Refractive error, diopters	−3.09 ± 2.63
Visual acuity, logMAR	0.20 ± 0.34
Foveal retinal thickness, μm	259.2 ± 143.6
Foveal choroidal thickness, μm	110.6 ± 68.7
Choroidal thickness of the central area within a circle of 1-mm diameter, μm	116.7 ± 60.6
Macular choroidal thickness within a circle of 6-mm diameter, μm	120.9 ± 53.0
Choroidal volume of the central area, mm^3	0.092 ± 0.048
Macular choroidal volume, mm^3	3.417 ± 1.500

logMAR, logarithm of minimal angle of resolution.

Choroidal Thickness and Volume Measurement Protocol

The choroidal thickness was defined as the distance between the outer border of the RPE and the choriosclera border. When the RPE was defective, as was seen sometimes in group 3, Bruch's membrane was considered to be an inner border of the choroid. In each of the 128 images of the data set, lines of both the RPE and the choriosclera border were segmented manually by a trained observer in a masked fashion; automated built-in calibration software determined the distance between these two lines. From the 128 segmented images of each data set, a choroidal thickness map of a 6 × 6-mm^2 area was created, and then the Early Treatment Diabetic Retinopathy Study grid[32] was applied to the map. In the current study, the central area and the macula were defined as areas within a circle of 1-mm and 6-mm diameter, respectively, centered on the fovea.

Using the averaged OCT images, we also measured the retinal thickness and the choroidal thickness at the center of the fovea. Foveal retinal thickness was defined as the distance between the vitreoretinal interface and the outer surface of RPE.

Statistical Analysis

Statistical analysis was performed using statistical software (SPSS 16; SPSS Inc., Chicago, IL). All values are presented as mean ± SD. The measured VA was converted to the logarithm of the minimum angle of resolution (logMAR) for statistical analysis. The data were analyzed using one-way analysis of variance with Tukey's post-hoc analysis to compare mean choroidal thickness at different regions. To compare the thickness within each group, two-way analysis of variance was used. Bivariate relationships were analyzed using the Pearson's correlation coefficient. A P value of less than 0.05 was considered to be statistically significant.

Results

In the current study, 42 eyes (32 patients, 9 men and 23 women; ranging in age from 42 to 87 years, mean 67.8 ± 11.3 years) with IPS were examined. Mean refractive error was −3.09 ± 2.63 diopters (range −0.25 to −10.0 diopters) and mean axial length was 25.00 ± 1.52 mm (range: 22.66–28.62 mm). Mean VA in logMAR was 0.20 ± 034 (range −0.18 to 1.30). Thirty five eyes (83.3%) showed a tilted disc (Table 1).

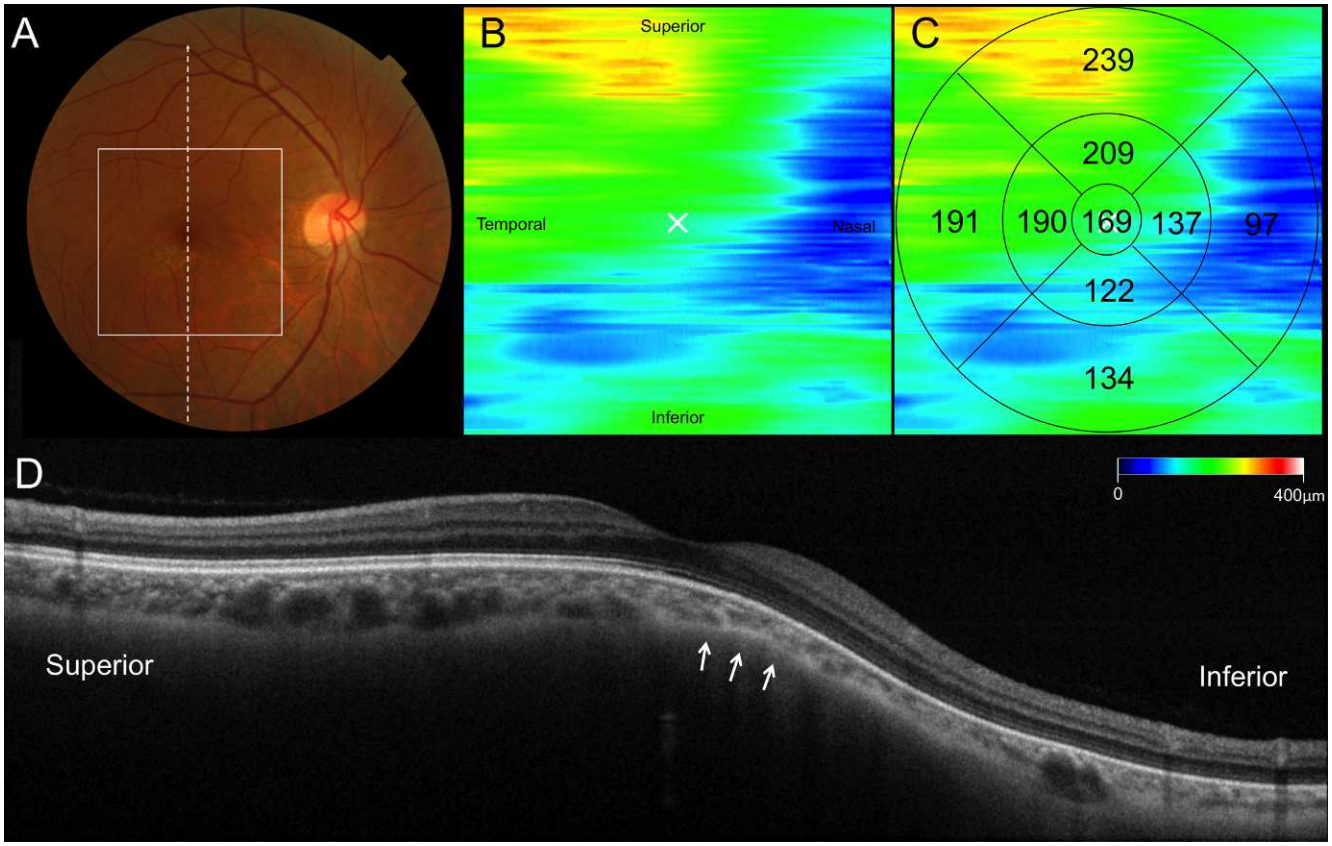

Figure 1. IPS without exudative complications. (**A**) Fundus photograph of the right eye of a 46-year-old woman shows a tilted disc, inferior crescent, and IPS, of which the superior border lies across the macula. VA was 20/13, refractive error was −1.25 diopters, and axial length was 24.17 mm. (**B**) Choroidal thickness map of the macula (6×6 mm^2) depicted in the fundus photograph obtained with swept source OCT at 1 μm. The map shows a belt-shaped area of substantially decreased choroidal thickness along the superior border of the IPS. The choroid in the inferior-nasal quadrant (within the staphyloma) is thinner than is the superior-temporal quadrant (outside the staphyloma). (**C**) Mean choroidal thickness in each sector of the Early Treatment Diabetic Retinopathy Study grid. (**D**) A multi-averaged vertical OCT image of 12 mm along the *dotted white arrow* in the fundus photograph. In the superior macula, a layer of medium diameter blood vessels and an outermost layer of the choroid consisting of larger-diameter blood vessels are seen. The choroid in the inferior macula within the staphyloma seems to be thin and the configuration of choroidal vascular layers is difficult to determine. *White cross* indicates the fovea. *Arrows* indicate the superior border of the IPS.

The Choroid in Eyes with IPS

Swept source OCT at 1-μm wavelength allows visualization of the clear structure of the posterior pole as well as allowing deeper penetration into the choroid. Multiaveraged scans revealed the configuration of the IPS and showed the superior border of the staphyloma, which lay across the macula. Figure 1 shows a typical case of IPS. In the superior macula, a layer of medium diameter blood vessels (Sattler's layer) and an outermost layer of the choroid consisting of larger-diameter blood vessels (Haller's layer) were identified. In many cases, however, the choroid in the inferior macula within the staphyloma was remarkably thin compared to the superior macula, and the configuration of choroidal vascular layers was difficult to discern.

Using a raster scan protocol, we created a choroidal thickness map. Of the 42 eyes with IPS, the mean macular choroidal thickness (within a circle of 6.0-mm diameter) was 120.9 ± 53.0 μm, but there were regional differences. The superior-temporal choroid (outside of the staphyloma) was well preserved, but the inferior-nasal choroid (within the staphyloma) appeared to be substantially thinned. Mean choroidal thickness of the inferior quadrant (101.5 ± 47.0 μm) was significantly less than that in the superior quadrant (155.5 ± 69.5 μm, $P < 0.001$) (Table 2). In addition, the choroidal thickness map revealed that the belt-shaped area

Table 2. Regional Choroidal Thickness of Eyes with Inferior Posterior Staphyloma within the Early Treatment Diabetic Retinopathy Grid

	Mean Choroidal Thickness, μm (P*)
Central area	116.7 ± 60.6
Inner sectors	
Inner superior sector	143.7 ± 68.0
Inner nasal sector	100.7 ± 47.8 (0.006)
Inner inferior sector	105.5 ± 53.6 (0.019)
Inner temporal sector	129.5 ± 66.1 (0.692)
Outer sectors	
Outer superior sector	159.3 ± 70.2
Outer nasal sector	85.9 ± 37.4 (<0.001)
Outer inferior sector	100.5 ± 45.7 (<0.001)
Outer temporal sector	140.2 ± 70.0 (0.475)
Quadrants	
Superior quadrant	155.5 ± 69.5
Nasal quadrant	89.2 ± 39.0 (<0.001)
Inferior quadrant	101.5 ± 47.0 (<0.001)
Temporal quadrant	137.7 ± 69.4 (0.538)

* Compared with values in the superior sectors or quadrants.

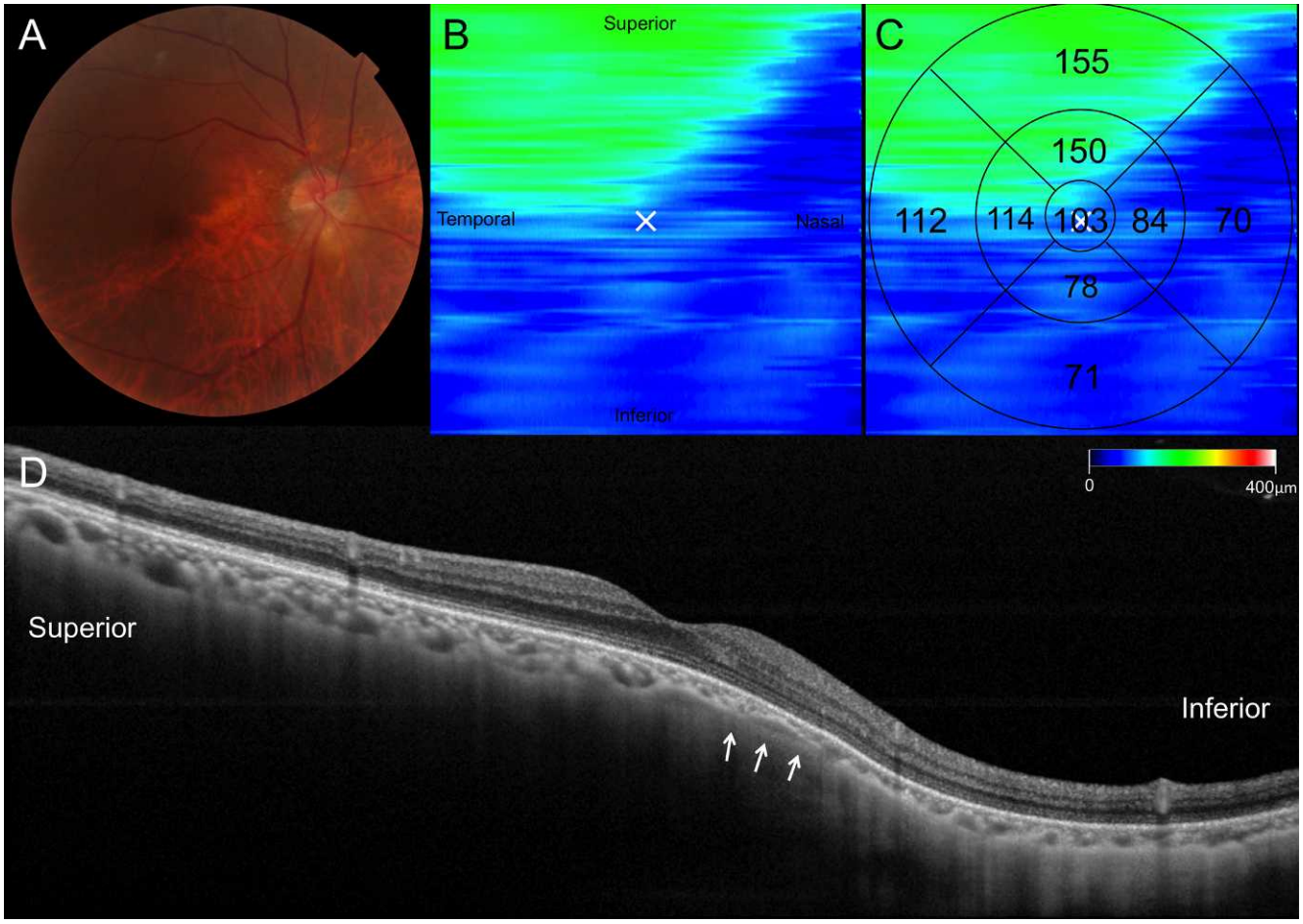

Figure 2. IPS of an older patient. (**A**) Fundus photograph of the right eye of 76-year-old man shows a tilted disc and IPS, of which the superior border lies across the macula. VA was 20/13, refractive error was −1.50 diopters, and axial length was 25.68 mm. (**B**) Macular choroidal thickness map obtained with swept source OCT at 1 μm. The macular choroidal thickness is reduced not only within the staphyloma but also in the entire macular area. Mean choroidal thickness is less than that in Figure 1. (**C**) Mean choroidal thickness was obtained for each sector. (**D**) A multiaveraged vertical OCT scan showing regional changes in choroidal thickness. *White cross* indicates the fovea. *Arrows* indicate the superior border of the IPS.

with markedly thinned choroid was consistent with the superior border of the staphyloma (Fig. 1).

Figure 2 shows a typical case of IPS in an older patient. As age increases, the macular choroidal thickness becomes reduced in the entire macular area; in eyes with IPS, the mean macular choroidal thickness showed a close correlation with age ($R^2 = 0.506$, $P < 0.001$) (Fig. 3). The foveal choroidal thickness, mean choroidal thickness of the central area (within

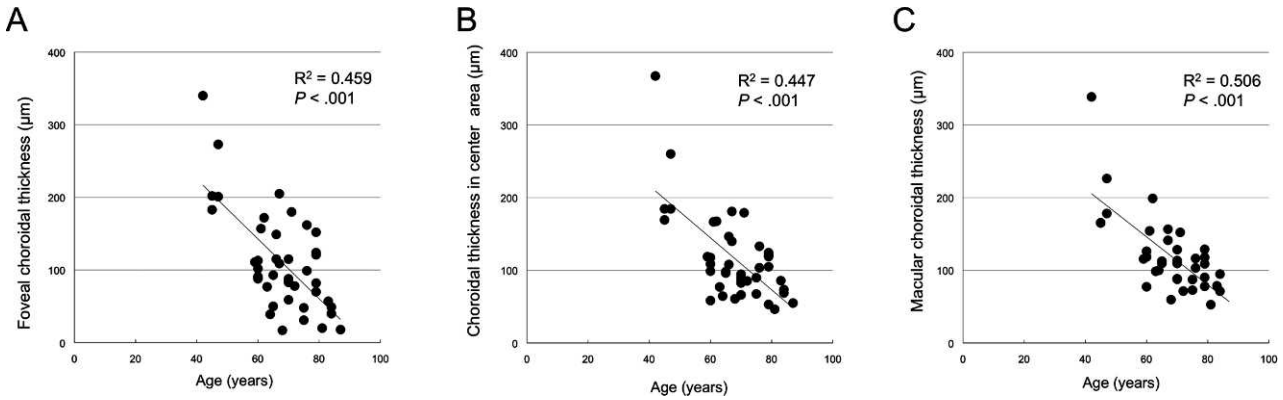

Figure 3. Scatter plots of the correlation between the choroidal thickness and age in eyes with IPS. (**A**) The foveal choroidal thickness is determined at the center of the fovea. (**B**) Choroidal thickness in central area is determined within a circle of 1-mm diameter centered on the fovea. (**C**) Macular choroidal thickness is determined within a circle of 6-mm diameter centered on the fovea. Foveal choroidal thickness, choroidal thickness in central area, and macular choroidal thickness were estimated to be decreased by 41.1 μm, 35.8 μm, and 33.0 μm per decade, respectively.

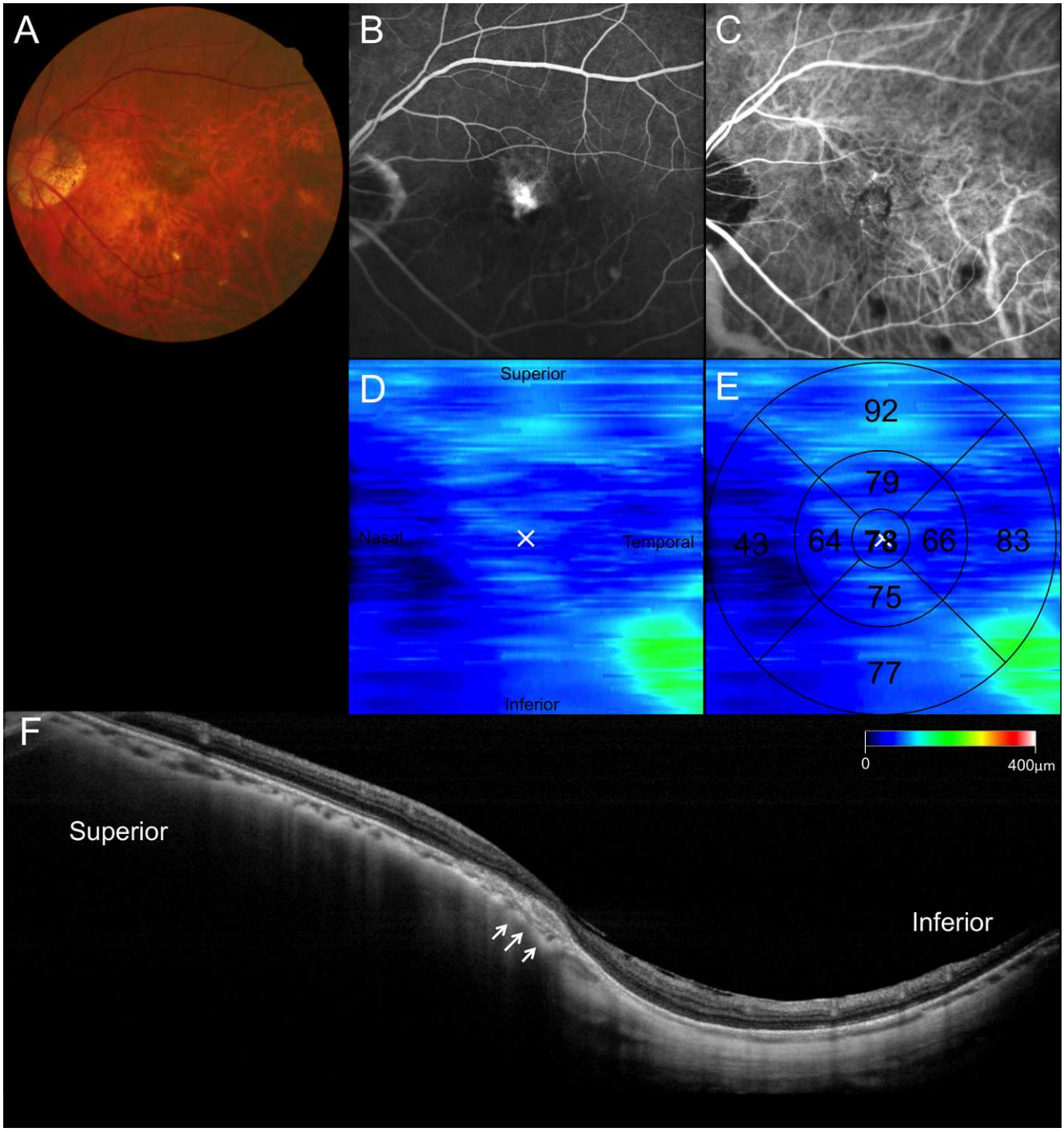

Figure 4. IPS with CNV. (**A**) Fundus photograph of the left eye of a 75-year-old woman shows IPS, of which the superior border lies across the macula. VA was 20/50, and axial length was 26.80 mm. This eye had been treated previously with three sessions of PDT. (**B**, **C**) Fluorescein and indocyanine green angiograms show CNV at the superior border of the IPS. (**D**) Macular choroidal thickness map obtained with swept source OCT at 1 μm. Choroidal thickness is substantially reduced not only at the center, where PDT was previously applied, but in the entire macular area. (**E**) Mean choroidal thickness was obtained for each sector. (**F**) A multi-averaged vertical OCT scan shows CNV on the border of the IPS (*arrows*) and choroidal thinning, especially within the IPS.

a circle of 1.0-mm diameter), and macular choroidal thickness were estimated to be decreased by 41.1 μm, 35.8 μm, and 33.0 μm per decade, respectively.

Complications Associated with IPS

Of the 42 eyes with IPS, 21 eyes (50%) showed no complication (group 1) (Figs. 1, 2), but the other half (21 eyes) (50%) had exudative complications at the superior border of the staphyloma. At the superior border of the staphyloma, CNV was seen in four eyes (9.5%) and PCV was seen in 4 eyes (9.5%) (group 3, $n = 8$) (Fig. 4). Of eyes without these neovascular complications (group 2, $n = 13$), six eyes (14.3%) showed a serous retinal detachment beneath the fovea (Fig. 5) and seven (16.7%) showed a small serous pigment epithelial detachment around the fovea (Fig. 6). VA was well

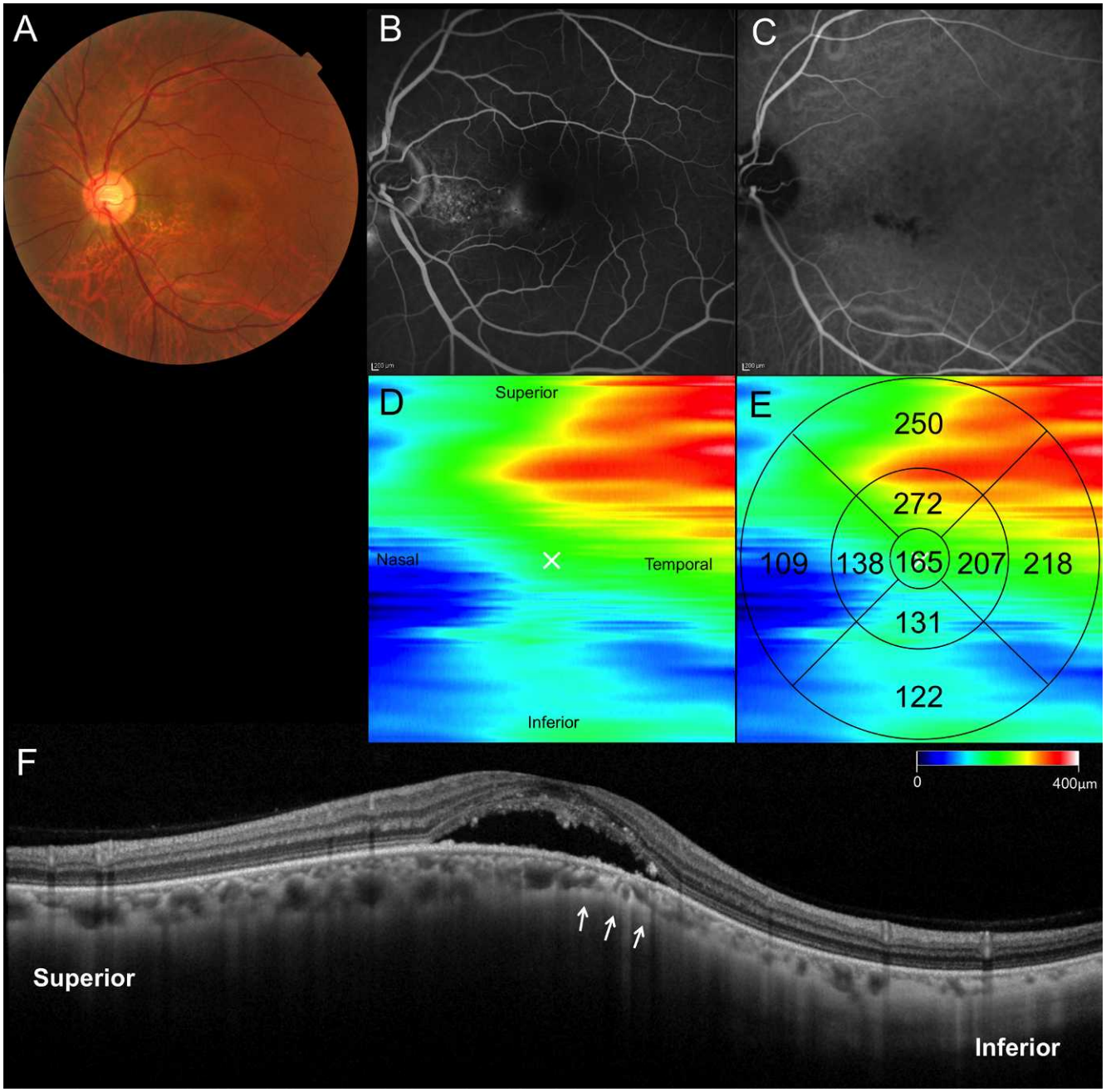

Figure 5. IPS with serous retinal detachment. (**A**) Fundus photograph of the left eye of a 47-year-old woman shows IPS, of which the superior border lies across the macula. VA was 20/20, and refractive error was −4.75 diopters. (**B**) Late-phase fluorescein angiogram shows multiple pinpoint staining. (**C**) Late-phase indocyanine green angiography confirms the absence of CNV. (**D**) Macular choroidal thickness map obtained with swept source OCT at 1 μm. (**E**) Mean choroidal thickness in each sector of the Early Treatment Diabetic Retinopathy Study grid. The choroidal thickness is preserved outside the staphyloma but is relatively thin within the IPS. (**F**) A multi-averaged vertical OCT scan shows the serous retinal detachment along the superior border of the IPS (*arrows*) and choroidal thinning within the IPS.

preserved in group 1 (0.01 ± 0.21) and was relatively well preserved in group 2 (0.21 ± 0.25). However, it was significantly reduced in group 3 (0.66 ± 0.33, $P < 0.001$). No eyes in groups 1or 2 had received any previous treatment. In group 3, three eyes had received anti-vascular endothelial growth factor (VEGF) therapy, two eyes had undergone photodynamic therapy (PDT), and three eyes had received combined anti-VEGF therapy and PDT for neovascular complications.

There were no differences in axial length, refractive error, or foveal retinal thickness between the three groups (Table 3). However, the mean age of patients in group 3 (76.4 ± 6.7 years) was older than that in group 1 (67.5 ± 12.4 years, $P=0.120$) or in group 2 (63.1 ± 9.1 years, $P=0.021$). Macular choroidal volume was 3.759 ± 1.748 mm^3 in group 1, 3.578 ± 0.842 mm^3 in group 2, and 2.163 ± 0.562 mm^3 in group 3, so it was significantly reduced in group 3 compared to group 1 ($P=0.035$).

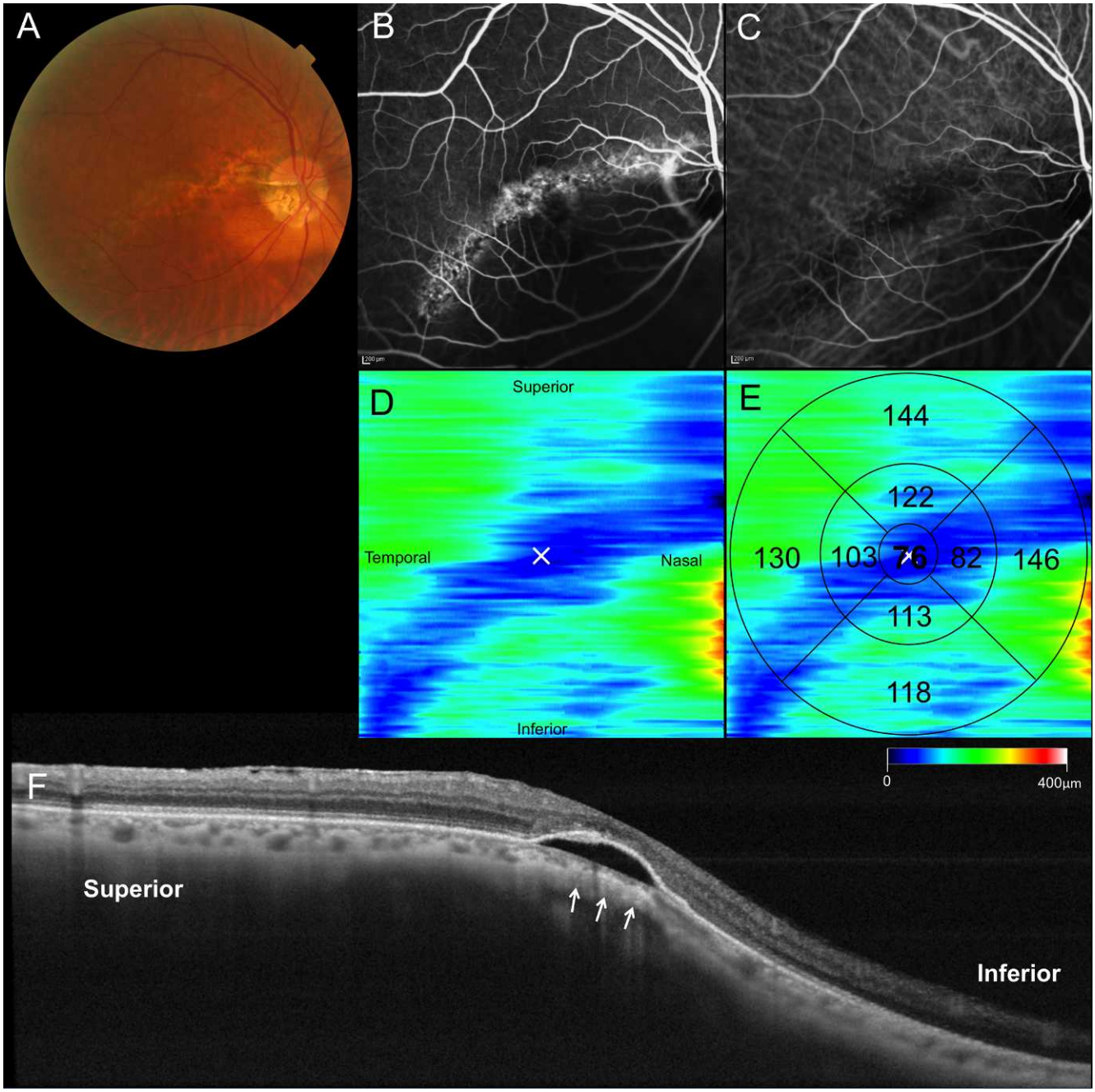

Figure 6. IPS with serous pigment epithelial detachment. (**A**) Fundus photograph of the right eye of a 70-year-old woman shows a tilted disc, inferior peripapillary crescent, and IPS, of which the superior border lies across the macula. Atrophic changes of the retinal pigment epithelium are observed along the border of the IPS. VA was 20/16, refractive error was −1.25 diopter, and axial length was 24.58 mm. (**B**) Fluorescein angiogram shows a belt-shaped area of granular hyperfluorescence corresponding to the border of the IPS. (**C**) Indocyanine angiogram confirms the absence of CNV. (**D**) Macular choroidal thickness map obtained with swept source OCT at 1 μm. The map shows a belt-shaped area of decreased choroidal thickness along the superior border of the IPS. (**E**) Mean choroidal thickness in each sector of the Early Treatment Diabetic Retinopathy Study grid. (**F**) A multi-averaged vertical OCT scan shows the serous pigment epithelial detachment with marked choroidal thinning on the superior border of the IPS (*arrows*).

Choroidal Thickness in the Macular Area of Each Group

Foveal choroidal thickness was 130.7 ± 74.4 μm in group 1, 118.8 ± 52.7 μm in group 2, and 44.6 ± 27.8 μm in group 3 (Table 3), indicating that it was significantly thinner in group 3 than in group 1 ($P = 0.005$) or group 2 ($P = 0.029$). Macular choroidal thickness was 133.0 ± 61.9 μm in group 1, 126.6 ± 29.2 μm in group 2, and 76.5 ± 19.9 μm in group 3. In group 2, macular choroidal thickness was almost the same at that in group 1, but was significantly reduced in group 3 compared with group 1 ($P = 0.035$). In group 3, the reduction in choroidal thickness was seen in most sectors of the ETDRS grid (Table 4). Table 5 shows the angiographic characteristics along the border of the IPS in each study group.

Table 3. Characteristics of Eyes and Mean Choroidal Thickness and Volume Obtained in Each Study Group

	Group 1 No Exudative Complications	Group 2 SRD or PED Only	Group 3 Neovascular Complications	*P* Value
Number of eyes	21	13	8	
Sex (male/female)	8/13	3/10	2/6	0.788
Tilted disc (%)	17 (81.0%)	10 (76.9%)	8 (100%)	0.355
Age, y	67.5 ± 12.4	63.1 ± 9.1	76.4 ± 6.7	0.028
Axial length, mm	25.2 ± 1.64	24.33 ± 0.50	25.48 ± 2.03	0.173
Refractive error, diopters	−3.01 ± 2.47	−2.25 ± 1.59	−4.64 ± 3.80	0.126
Visual acuity, logMAR	0.01 ± 0.21	0.21 ± 0.25	0.66 ± 0.33*	<0.001
Foveal retinal thickness, μm	214.9 ± 58.1	270.5 ± 152.5	357.3 ± 232.7	0.051
Foveal choroidal thickness, μm	130.7 ± 74.4	118.8 ± 52.7	44.6 ± 27.8*	0.006
Macular choroidal thickness, μm	133.0 ± 61.9	126.6 ± 29.2	76.5 ± 19.9†	0.042
Macular choroidal volume, mm^3	3.759 ± 1.748	3.578 ± 0.824	2.163 ± 0.562†	0.042

SRD, serous retinal detachment; PED, pigment epithelial detachment; logMAR, logarithm of minimal angle of resolution. All values were compared using one-way analysis of variance with Tukey's post-hoc analysis.

* $P < 0.01$, † $P < 0.05$, compared with group 1.

Regional Choroidal Thickness

Table 6 shows the mean choroidal thickness of each quadrant of the macula in the three groups. In groups 1 and 2, the choroidal thickness in the inferior-nasal quadrants was significantly reduced compared with that in the superior quadrant ($P < 0.001$). In group 3, however, the choroidal thickness was decreased throughout the entire macular area.

Association of Age and Macular Choroidal Thickness

Figure 7 shows the association of age and macular choroidal thickness in each group. Most eyes in group 3 appeared to be older and to have a thin macular choroid. We further analyzed only patients who were 70 years of age or older in each group. In these patients, eyes in group 3 had a significantly thinner macular choroid (79.4 ± 20.2 μm) than did eyes in groups 1 or 2 (105.4 ± 22.3 μm, $P = 0.024$).

Discussion

In most previous reports, the choroidal thickness was measured at the foveal center. In most pathologic eyes, including those with IPS, the choroid would show regional changes in thickness, and if measured from a single A-scan, may be influenced by irregularity or by focal indistinctness of the chorioscleral border. In addition, when eyes with IPS are scanned with a conventional spectral domain OCT, the obtained images may be partially inverted due to the limit of the scan window. In the current study, the macular area was studied with a swept source OCT at 1050 nm. With the use of a light source at a longer wavelength, the currently used swept source OCT allows high-contrast imaging of the entire choroid. In addition, the tunable laser source of the swept source OCT has lower signal decay versus depth than do the existing spectral domain OCT systems. Having a long scan window depth, the swept source OCT used in the current study allowed entire line scans of 12 mm, even in eyes with IPS.

With these advantages, the current study has revealed that eyes with IPS showed a relatively well-preserved choroid away from the staphyloma, but that the inferior-nasal choroid within the staphyloma was thinned substantially. In addition, eyes with IPS often have a belt-shaped area with the thinnest choroid being at the superior border of the staphyloma. As age increases, however, the choroidal thinning progresses, and ultimately involves the entire macular area. In our patients, 50% of the eyes with IPS had exudative complications at the superior border of the staphyloma. Eyes with only serous retinal detachment or pigment epithelial detachment had a preserved choroid and maintained a good VA. However, most eyes that had developed neovascular complications had a

Table 4. Choroidal Thickness in Each Sector of Early Treatment Diabetic Retinopathy Grid in Each Study Group

	Mean Choroidal Thickness, μm		
Sectors	Group 1 No Exudative Complications	Group 2 SRD or PED Only	Group 3 Neovascular Complications
Central area (*P**)	132.8 ± 72.6	117.7 ± 43.3 (0.742)	73.1 ± 18.0 (0.045)
Inner superior (*P**)	161.2 ± 75.2	155.4 ± 50.6 (0.962)	78.8 ± 24.0 (0.007)
Inner nasal (*P**)	112.7 ± 56.0	105.9 ± 33.3 (0.901)	60.6 ± 14.1 (0.020)
Inner inferior (*P**)	113.9 ± 66.7	114.0 ± 32.2 (1.000)	69.4 ± 22.3 (0.111)
Inner temporal (*P**)	145.3 ± 80.0	134.8 ± 38.5 (0.884)	79.3 ± 33.0 (0.040)
Outer superior (*P**)	178.9 ± 78.1	165.2 ± 44.0 (0.843)	91.9 ± 19.7 (0.010)
Outer nasal (*P**)	94.7 ± 41.1	89.2 ± 29.5 (0.914)	54.8 ± 15.6 (0.035)
Outer inferior (*P**)	104.8 ± 56.1	112.7 ± 20.0 (0.887)	70.0 ± 20.1 (0.187)
Outer temporal (*P**)	154.1 ± 83.5	146.1 ± 38.5 (0.949)	89.9 ± 32.2 (0.088)

Mean choroidal thickness in each sector was compared using one-way analysis of variance with Tukey's post-hoc analysis.

* *P*, compared with group 1.

Table 5. Angiographic Characteristics along the Border of the Inferior Posterior Staphyloma in Each Study Group*

	Group 1 No Exudative Complications	Group 2 SRD or PED Only	Group 3 Neovascular Complications
Fluorescein angiography	16	13	8
Window defect	8	11	7
Pinpoint hyperfluorescence	1	13	0
Indocyanine green angiography	15	12	7
Pinpoint hyperfluorescence	0	4	0
Late wide hyperfluorescence	5	12	2
Choroidal hyperpermeability	1	1	0

* Fluorescein angiography was not performed in five eyes with no exudative complications, and indocyanine green angiography was not performed in six eyes with no exudative complications. Each characteristic was defined according to the previous report by Nakanishi et al.[7]

thinner macular choroid than did eyes without such complications.

In our patients with IPS, the mean macular choroidal thickness was 120.9 ± 53.0 μm. One of the most significant limitations of the current study was the lack of controls. To date, there is limited information on the macular choroidal thickness of normal eyes. With swept source OCT at 1060 nm, Agawa et al.[33] reported the mean macular choroidal thickness in healthy subjects to be 348 ± 63 μm. However, the age of subjects in their study (32.9 ± 8.5 years) was much younger than our patients (67.8 ± 11.3 years). Recently, Hirata et al.[30] reported the macular choroidal thickness of healthy subjects examined with the same protocol and OCT machine used in the current study. Table 7 shows the data on normal subjects with an age greater than 40 years that was extracted from their report. In our patients with IPS, macular choroidal thickness was reduced significantly compared with normal subjects in their report (choroidal thickness, 186.6 ± 72.4 μm; mean age, 70.1 ± 10.0 years).

Recently, Yamagishi et al.[34] reported marked choroidal thinning at the superior border in five eyes with a serous detachment due to IPS, and they speculated that decreased ability of the choroid to remove the subretinal fluid may be responsible for the development of such a serous retinal detachment. In our patients in group 2, the choroidal thickness map revealed the belt-shaped area with substantially thinned choroid. However, the macular choroidal thickness in group 2 patients was as thick as was that in group 1 patients. In eyes with IPS, Maruko et al.[22] recently described choroidal thinning and scleral thickening of the fovea, and they speculated that choroidal fluid within the IPS might not pass through a thickened sclera and could leak into the subretina through degenerated RPE. In our patients, seven eyes showed a small serous pigment epithelial detachment around the fovea, and impaired flow in the choroid could lead to fluid accumulation within Bruch's membrane, and result in the formation of a pigment epithelial detachment. Even with the use of swept source OCT at a longer wavelength, however, we could not determine the outer border of the sclera in all cases, especially in those eyes in which the RPE was preserved.

In the current study, eyes that developed neovascular complications had a much thinner macular choroid than did those without such complications. However, the mean age of patients with these neovascular complications was older by 8.9 years compared to patients without complications. Previously, Margolis and Spaide[35] reported that the subfoveal choroidal thickness decreased by 15.6 μm per decade in normal eyes, and Fujiwara et al.[24] reported that subfoveal choroidal thickness decreased by 12.7 μm per decade in highly myopic eyes, so we believed that the choroidal thinning in our group 3 patients could not be fully explained by age alone. In addition, when comparing only patients over age 70 years, eyes with neovascular complications had a significantly thinner macular choroid than did those without any complication. Indeed, although eyes with IPS may show progressive thinning of the choroid over time, it is possible that eyes with IPS have a wide range of choroidal thicknesses, and that eyes with a thinner choroid tend to develop CNV.

Ikuno et al.[36] reported that choroidal thinning is associated with the development of myopic CNV, and Chung et al.[14] reported reduced choroidal thickness in eyes with neovascular age-related macular degeneration. Although choroidal thinning is recognized as a risk for the development of CNV, its precise mechanism has not been fully elucidated. Goldberg et al.[37] reported that most CNV in age-related macular degeneration occurs close to areas with poor choroidal perfusion on indocyanine green angiography. Hayashi and de Laey[38] postulated that hypoxic regions of the choroid are the underlying cause of CNV. In eyes with IPS, the choroidal thinning may also be involved in the development of CNV by the focal choroidal ischemia and concomitant poor choroidal perfusion. Previously, Nakanishi et al.[7] reported that eyes with IPS often show hypofluorescence due to atrophy of the choriocapillaris in the early phase of indocyanine green angiography. In eyes with IPS, atrophy of the choriocapillaris may also cause focal hypoxic stress.

Table 6. Mean Choroidal Thickness in Each Quadrant Obtained with Swept Source Optical Coherence Tomography

		Mean Choroidal Thickness of Each Quadrant, μm			
		Superior	Inferior	Temporal	Nasal
Group 1	No complications (*P**)	174.8 ± 76.9	106.9 ± 57.7 (<0.001)	152.1 ± 82.5 (0.072)	98.8 ± 43.9 (<0.001)
Group 2	SRD or PED only (*P**)	161.5 ± 45.7	111.6 ± 22.7 (<0.001)	142.5 ± 38.6 (0.265)	91.7 ± 28.0 (<0.001)
Group 3	Neovascular complications (*P**)	89.0 ± 20.3	70.9 ± 19.7 (0.126)	87.7 ± 32.6 (0.998)	56.7 ± 14.4 (0.003)

Mean choroidal thickness in each quadrant was compared using two-way analysis of variance with Tukey's post-hoc analysis.
* *P*, compared with values in superior quadrant.

Table 7. Choroidal Thickness of Eyes of Normal Subjects Greater than 40 Years Old and of Eyes with Inferior Posterior Staphyloma

	Normal Eyes More than 40 Years Old*	Inferior Posterior Staphyloma	*P* Value
Number of eyes	27	42	
Age, y	70.1 ± 10.0	67.8 ± 11.3	0.384
Axial length, mm	24.23 ± 1.84	25.00 ± 1.52	0.083
Refractive error, diopters	−1.76 ± 4.96	−3.09 ± 2.62	0.217
Foveal choroidal thickness, μm	200.2 ± 79.7	110.6 ± 68.7	<0.001
Choroidal thickness			
of the central area, μm	199.1 ± 80.5	116.7 ± 60.6	<0.001
of the macula, μm	186.6 ± 72.4	120.9 ± 53.0	<0.001
in the superior quadrant, μm	209.0 ± 79.3	155.5 ± 69.5	0.005
in the inferior quadrant, μm	183.5 ± 72.9	101.5 ± 47.0	<0.001

* Normal eyes older than 40 years were extracted from the report by Hirata and associates.[30]

It is possible that previous treatments were involved in the choroidal thinning seen in group 3. Previous reports showed that subfoveal choroidal thickness was decreased after PDT in eyes with PCV.[15] In eyes treated with PDT (group 3), the choroid was significantly reduced throughout the macula, not only in the region where the laser irradiation had been performed. Anti-VEGF treatments also may have been involved in the thinner choroid in group 3. Recently, Yamazaki et al.[39] reported that in eyes with exudative age-related macular degeneration treated with ranibizumab, mean subfoveal choroidal thickness decreases from 244 μm at baseline to 226 μm at 12 months. Although those authors found a statistically significant decrease in the foveal choroidal thickness, the mean reduction was only 18 μm. Based on these evidences, previous treatment does not explain sufficiently the decrease in macular choroidal thickness in eyes with neovascular complications.

The current study certainly had limitations, including lack of a control group and the fact that it is descriptive in nature. In addition, the sample size in each subgroup was relatively small. We categorized eyes with serous retinal detachment or pigment epithelial detachment into one group, and eyes with PCV or CNV into another group for statistical analysis. Furthermore, in the current study, described herein, both RPE line and chorioscleral border were segmented manually. In addition, this study showed only the macular choroidal thickness, not the function of the choroid. Most significant of all, because this was a cross-sectional study, it was difficult to determine whether choroidal thinning was a cause or a consequence of the development of CNV. Further longitudinal prospective studies are needed to elucidate the role played by the choroid in the development of CNV in eyes with IPS.

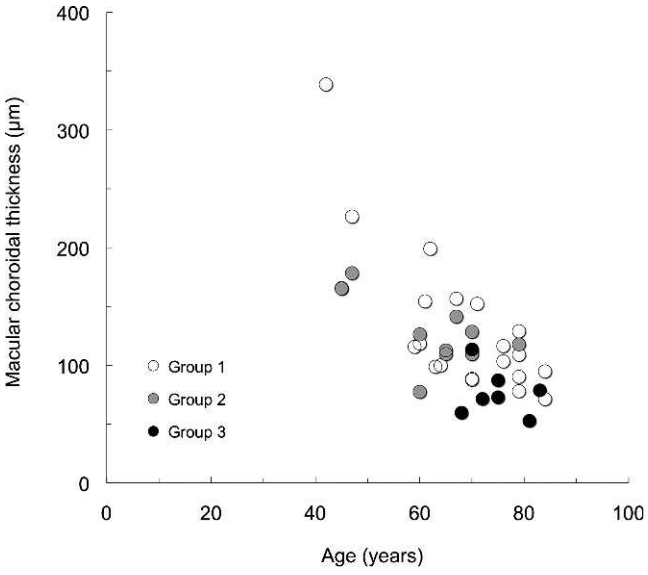

Figure 7. Scatter plot showing correlation between the macular choroidal thickness and patient age in eyes with IPS. Most eyes in group 3 are older and have a thin macular choroid.

References

1. Curtin BJ. The posterior staphyloma of pathologic myopia. *Trans Am Ophthalmol Soc*. 1977;75:67–86.
2. Apple DJ, Rabb MF, Walsh PM. Congenital anomalies of the optic disc. *Surv Ophthalmol*. 1982;27:3–41.
3. Dorrell D. The tilted disc. *Br J Ophthalmol*. 1978;62:16–20.
4. Witmer MT, Margo CE, Drucker M. Tilted optic disks. *Surv Ophthalmol*. 2010;55:403–428.
5. Riise D. The nasal fundus ectasia. *Acta Ophthalmol Suppl*. 1975;(126):3–108.
6. Cohen SY, Quentel G, Guiberteau B, Delahaye-Mazza C, Gaudric A. Macular serous retinal detachment caused by subretinal leakage in tilted disc syndrome. *Ophthalmology*. 1998;105:1831–1834.
7. Nakanishi H, Tsujikawa A, Gotoh N, et al. Macular complications on the border of an inferior staphyloma associated with tilted disc syndrome. *Retina*. 2008;28:1493–1501.
8. Leys AM, Cohen SY. Subretinal leakage in myopic eyes with a posterior staphyloma or tilted disk syndrome. *Retina*. 2002; 22:659–665.
9. Tsuboi S, Uchihori Y, Manabe R. Subretinal neovascularisation in eyes with localised inferior posterior staphylomas. *Br J Ophthalmol*. 1984;68:869–872.
10. Mauget-FaŸsse M, Cornut PL, Quaranta El-Maftouhi M, Leys A. Polypoidal choroidal vasculopathy in tilted disk syndrome and high myopia with staphyloma. *Am J Ophthalmol*. 2006;142: 970–975.
11. Theodossiadis PG, Grigoropoulos V, Emfietzoglou J, Theodossiadis GP. Optical coherence tomography study of tilted optic disk associated with macular detachment. *Graefes Arch Clin Exp Ophthalmol*. 2006;244:122–124.
12. Stur M. Congenital tilted disk syndrome associated with parafoveal subretinal neovascularization. *Am J Ophthalmol*. 1988;105:98–99.
13. Cohen SY, Dubois L, Ayrault S, Quentel G. T-shaped pigmentary changes in tilted disk syndrome. *Eur J Ophthalmol*. 2009;19:876–879.
14. Chung SE, Kang SW, Lee JH, Kim YT. Choroidal thickness in polypoidal choroidal vasculopathy and exudative age-related macular degeneration. *Ophthalmology*. 2011;118:840–845.

15. Maruko I, Iida T, Sugano Y, Saito M, Sekiryu T. Subfoveal retinal and choroidal thickness after verteporfin photodynamic therapy for polypoidal choroidal vasculopathy. *Am J Ophthalmol*. 2011;151:594–603.
16. Imamura Y, Fujiwara T, Margolis R, Spaide RF. Enhanced depth imaging optical coherence tomography of the choroid in central serous chorioretinopathy. *Retina*. 2009;29:1469–1473.
17. Koizumi H, Yamagishi T, Yamazaki T, Kawasaki R, Kinoshita S. Subfoveal choroidal thickness in typical age-related macular degeneration and polypoidal choroidal vasculopathy. *Graefes Arch Clin Exp Ophthalmol*. 2011;249:1123–1128.
18. Maruko I, Iida T, Sugano Y, Ojima A, Ogasawara M, Spaide RF. Subfoveal choroidal thickness after treatment of central serous chorioretinopathy. *Ophthalmology*. 2010;117:1792–1799.
19. Maruko I, Iida T, Sugano Y, et al. Subfoveal choroidal thickness after treatment of Vogt-Koyanagi-Harada disease. *Retina*. 2011; 31:510–517.
20. Spaide RF. Enhanced depth imaging optical coherence tomography of retinal pigment epithelial detachment in age-related macular degeneration. *Am J Ophthalmol*. 2009;147: 644–652.
21. Wood A, Binns A, Margrain T, et al. Retinal and choroidal thickness in early age-related macular degeneration. *Am J Ophthalmol*. 2011;152:1030–1038.
22. Maruko I, Iida T, Sugano Y, Oyamada H, Sekiryu T. Morphologic choroidal and scleral changes at the macula in tilted disc syndrome with staphyloma using optical coherence tomography. *Invest Ophthalmol Vis Sci*. 2011;52:8763–8768.
23. Spaide RF, Koizumi H, Pozzoni MC. Enhanced depth imaging spectral-domain optical coherence tomography. *Am J Ophthalmol*. 2008;146:496–500.
24. Fujiwara T, Imamura Y, Margolis R, Slakter JS, Spaide RF. Enhanced depth imaging optical coherence tomography of the choroid in highly myopic eyes. *Am J Ophthalmol*. 2009;148: 445–450.
25. Rahman W, Chen FK, Yeoh J, Patel P, Tufail A, Da Cruz L. Repeatability of manual subfoveal choroidal thickness measurements in healthy subjects using the technique of enhanced depth imaging optical coherence tomography. *Invest Ophthalmol Vis Sci*. 2011;52:2267–2271.
26. Shah SU, Kaliki S, Shields CL, Ferenczy SR, Harmon SA, Shields JA. Enhanced depth imaging optical coherence tomography of choroidal nevus in 104 cases. *Ophthalmology*. 2012;119: 1066–1072.
27. Chen FK, Yeoh J, Rahman W, Patel PJ, Tufail A, Da Cruz L. Topographic variation and interocular symmetry of macular choroidal thickness using enhanced depth imaging optical coherence tomography. *Invest Ophthalmol Vis Sci*. 2012;53: 975–985.
28. Vance SK, Imamura Y, Freund KB. The effects of sildenafil citrate on choroidal thickness as determined by enhanced depth imaging optical coherence tomography. *Retina*. 2011; 31:332–335.
29. Kim SW, Oh J, Kwon SS, Yoo J, Huh K. Comparison of choroidal thickness among patients with healthy eyes, early age-related maculopathy, neovascular age-related macular degeneration, central serous chorioretinopathy, and polypoidal choroidal vasculopathy. *Retina*. 2011;31:1904–1911.
30. Hirata M, Tsujikawa A, Matsumoto A, et al. Macular choroidal thickness and volume in normal subjects measured by swept-source optical coherence tomography. *Invest Ophthalmol Vis Sci*. 2011;52:4971–4978.
31. Ikuno Y, Maruko I, Yasuno Y, et al. Reproducibility of retinal and choroidal thickness measurements in enhanced depth imaging and high-penetration optical coherence tomography. *Invest Ophthalmol Vis Sci*. 2011;52:5536–5540.
32. Early Treatment Diabetic Retinopathy Study Research Group. Photocoagulation for diabetic macular edema. Early Treatment Diabetic Retinopathy Study report number 1. *Arch Ophthalmol*. 1985;103:1796–1806.
33. Agawa T, Miura M, Ikuno Y, et al. Choroidal thickness measurement in healthy Japanese subjects by three-dimensional high-penetration optical coherence tomography. *Graefes Arch Clin Exp Ophthalmol*. 2011;249:1485–1492.
34. Yamagishi T, Koizumi H, Yamazaki T, Kinoshita S. Choroidal thickness in inferior staphyloma associated with posterior serous retinal detachment. *Retina*. 2012;32:1237–1242.
35. Margolis R, Spaide RF. A pilot study of enhanced depth imaging optical coherence tomography of the choroid in normal eyes. *Am J Ophthalmol*. 2009;147:811–815.
36. Ikuno Y, Jo Y, Hamasaki T, Tano Y. Ocular risk factors for choroidal neovascularization in pathologic myopia. *Invest Ophthalmol Vis Sci*. 2010;51:3721–3725.
37. Goldberg MF, Dhaliwal RS, Olk RJ. Indocyanine green angiography patterns of zones of relative decreased choroidal blood flow in patients with exudative age-related macular degeneration. *Ophthalmic Surg Lasers*. 1998;29:385–390.
38. Hayashi K, de Laey JJ. Indocyanine green angiography of submacular choroidal vessels in the human eye. *Ophthalmologica*. 1985;190:20–29.
39. Yamazaki T, Koizumi H, Yamagishi T, Kinoshita S. Subfoveal choroidal thickness after ranibizumab therapy for neovascular age-related macular degeneration: 12-month results. *Ophthalmology*. 2012;119:1621–1627.